Rotational Symmetry Breaking in Sodium Doped Cuprates

Yan Chen¹, T. M. Rice^{1,2}, and F. C. Zhang¹

¹Department of Physics and Center of Theoretical and Computational Physics,

The University of Hong Kong, Pokfulam Road, Hong Kong, China

²Institut für Theoretische Physik, ETH-Zürich, CH-8093 Switzerland

(Dated: October 16, 2018)

Abstract

For reasonable parameters a hole bound to a Na⁺ acceptor in $Ca_{2-x}Na_xCuO_2Cl_2$ has a doubly degenerate ground state whose components can be represented as states with even (odd) reflection symmetry around the x(y)-axes. The conductance pattern for one state is anisotropic as the tip of a tunneling microscope scans above the Cu-O-Cu bonds along the x(y)-axes. This anisotropy is pronounced at lower voltages but is reduced at higher voltages. Qualitative agreement with recent experiments leads us to propose this effect as an explanation of the broken local rotational symmetry.

PACS numbers: 74.72.-h, 74.62.Dh, 74.25.Jb

The recent atomically resolved scanning tunneling microscopy (STM) studies by Davis and collaborators [1, 2] on strongly underdoped $Ca_{2-x}Na_xCuO_2Cl_2$ revealed a surprisingly complex pattern with the square symmetry of the lattice broken on a local scale. The STM data were analyzed to obtain the local hole density of Cu-site using the method proposed by Randeria, Sensarma, Trivedi and Zhang [3] and also a related method proposed by Anderson [4]. In these methods, the differential conductance signal is integrated from the chemical potential to a substantial voltage cutoff. Randeria *et al.* [3] pointed out that the ratio between its positive voltage (electron injection) and negative voltage (hole injection) signals measured the local hole density of the Cu-site independent of the strength of the troublesome tunneling matrix elements.

In $Ca_{2-x}Na_xCuO_2Cl_2$ the acceptor Na^+ -ions substitute for Ca^{2+} -ions and sit in the center of a square of four Cu sites both above and below the outermost CuO_2 layer. The attractive potential for the doped holes generated by a Na^+ acceptor does not break the local square symmetry. The local square lattice symmetry broken observed in the STM data is most pronounced at the in-plane oxygen sites and for the lower voltage cutoff. This has raised an interesting question about the origin of the broken local square symmetry in the STM experiments.

In this letter we address the origin of this broken local symmetry. We show that such

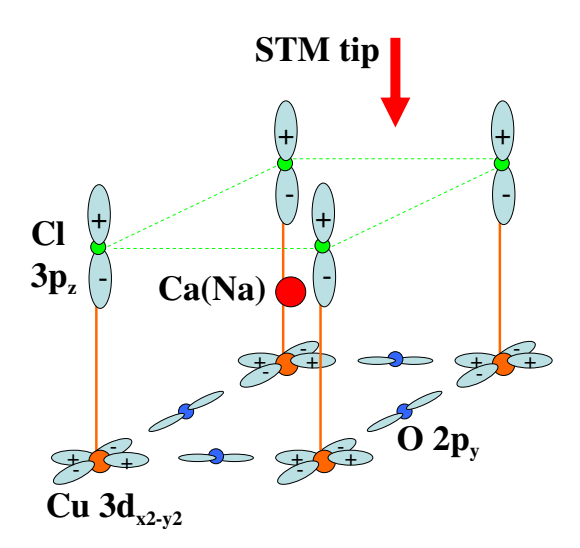


FIG. 1: Schematic crystal structure of $Ca_{2-x}Na_xCuO_2Cl_2$ around a Ca^{2+} ion or a doped Na^+ ion. The sign represents the phase of the Cu- and Cl-orbital wavefunction.

broken symmetry states appear in the case of a hole confined to a cluster of sites centered at a Na⁺-acceptor. Further this broken local symmetry shows up in the STM mapping primarily as a modulation pattern above the O-sites in the outermost CuO₂-layer.

We start by considering the STM tunneling process in detail in $\text{Ca}_{2-x}\text{Na}_x\text{CuO}_2\text{Cl}_2$. As pointed out by Rice and Tsunetsugu [5], the STM tip will couple primarily to the 3p_z-states of the outermost Cl layer but the matrix element for an electron to tunnel directly into a hole located on the CuO_2 square directly underneath the Cl-ion vanishes by symmetry. The holes move in a band of singlets in a state with $d_{x^2-y^2}$ -symmetry centered on a Cu-site but strongly hybridized with the four nearest-neighboring (n.n.) O sites that surround each Cu. The 3p_z-Cl states however hybridize with the hole states centered on the four n.n. Cu sites. Each of these states hybridizes either through the direct overlap of the 3p_z-Cl with 2p_{x(y)}-O orbitals and also through the 4s-Cu orbital on the site directly below each Cl. Let $|\Psi_0^{1h}\rangle$ denote the single hole ground state with energy E_0^{1h} , we can write the amplitude to inject an electron in a 3p_z-Cl hole wavefunction as a superposition in hole-states centered on the four n.n. Cu-site.

$$p_{Cl,\vec{i},\sigma}^{\dagger}|\Psi_{0}^{1h}\rangle \propto \sum_{\vec{\tau}} \langle \vec{i}, Cl|\vec{i} + \vec{\tau}, Cu\rangle c_{\vec{i}+\vec{\tau},\sigma}^{\dagger}|\Psi_{0}^{1h}\rangle$$

$$\propto \sum_{\vec{\tau}} (-1)^{M_{\vec{\tau}}} c_{\vec{i}+\vec{\tau},\sigma}^{\dagger}|\Psi_{0}^{1h}\rangle \tag{1}$$

where $p_{Cl,\vec{i},\sigma}^{\dagger}(c_{i+\vec{\tau},\sigma}^{\dagger})$ are creation operators for electrons in the $3p_z$ -Cl orbital at site i (planar coordinate) and the d-p hybridized orbital centered on the Cu-site at $\vec{i} + \vec{\tau}$ in the outermost CuO₂ layer respectively, $\vec{\tau} = \pm \hat{x}, \pm \hat{y}$ is a planar vector connecting n.n. Cu sites. $\langle \vec{i}, Cl | \vec{i} + \vec{\tau}, Cu \rangle$ denotes the overlap between a $3p_z$ -Cl and the d-p hybridized orbital centered at a n.n. Cu site. Assuming the square lattice is four-fold rotational invariant, the overlaps are independent of $\vec{\tau}$ except for their sign, which leads to the final result in Eqn. (1). For $d_{x^2-y^2}$ symmetry of the Cu-orbital, we have $(-1)^M = -1$ for $\vec{\tau} = \pm \hat{x}$, and $(-1)^M = +1$ for $\vec{\tau} = \pm \hat{y}$. Note that only the relative phase is important.

Following the theory of STM tunneling processes developed by Tersoff and Hamann [6], we can write the differential conductance at voltage V at \vec{r} , the center of curvature of the tip,

$$\frac{dI(\vec{r})}{dV} \propto \sum_{\sigma,m} |\langle m|a_{\vec{r},\sigma}^{\dagger}|\Psi_0^{1h}\rangle|^2 \delta_{E_m - E_0^{1h},\omega}$$
 (2)

where $a_{\vec{r},\sigma}^{\dagger}$ is the electron creation operator at position \vec{r} , $|m\rangle$ are eigenstates of the half-filled system with energy E_m , and $\omega = eV$. When the tip is scanned from above the Cl site at \vec{i} to a neighboring site, $\vec{i} + \vec{\tau'}$, (planar coordinates), we have

$$a_{\vec{r},\sigma}^{\dagger}|\Psi_{0}^{1h}\rangle = [\langle \vec{r}|\vec{i},Cl\rangle p_{Cl,\vec{i},\sigma}^{\dagger} + \langle \vec{r}|\vec{i} + \vec{\tau'},Cl\rangle p_{Cl,\vec{i}+\vec{\tau'},\sigma}^{\dagger}]|\Psi_{0}^{1h}\rangle. \tag{3}$$

The integrated current at \vec{r} up to a positive voltage V is then,

$$I(\vec{r},\omega) = A \sum_{\sigma,m} |\langle m| \sum_{\vec{\tau}} (-1)^{M_{\vec{\tau}}} [\langle \vec{r}|\vec{i},Cl\rangle c_{\vec{i}+\vec{\tau},\sigma}^{\dagger} + \langle \vec{r}|\vec{i}+\vec{\tau}',Cl\rangle c_{\vec{i}+\vec{\tau}'+\vec{\tau},\sigma}^{\dagger} |\Psi_{0}^{1h}\rangle|^{2} \Theta(\omega - E_{m} + E_{0}^{1h})$$

$$(4)$$

where A is a constant, and Θ is a step function. The variation of the tunneling current as one scans between two n.n. Cl sites will therefore be sensitive to the relative phase to inject electrons on n.n. Cu sites in $|\Psi_0^{1h}\rangle$. To this end we examine the lowest energy single-hole states for clusters up to 16 sites including an attractive potential for the center square.

The two-dimensional single-band t-t'-J model with the on-site impurity potential on four Cu sites of the center square around the Na⁺ dopant is defined by the Hamiltonian,

$$\mathcal{H} = -\sum_{i,\sigma} \epsilon_i c_{i\sigma}^{\dagger} c_{i\sigma} - t \sum_{\langle i,j \rangle \sigma} (c_{i\sigma}^{\dagger} c_{j\sigma} + \text{h.c.})$$
$$-t' \sum_{\langle \langle i,j \rangle \rangle \sigma} (c_{i\sigma}^{\dagger} c_{j\sigma} + \text{h.c.}) + J \sum_{\langle i,j \rangle} \mathbf{S}_i \cdot \mathbf{S}_j.$$
(5)

A constraint of no double electron occupation is implied. $\langle i,j \rangle$ and $\langle \langle i,j \rangle \rangle$ refer to n.n. and next n.n. sites i and j. The onsite potential of the four n.n. Cu sites around the sodium dopant is $\epsilon_i = \epsilon_s$ while $\epsilon_i = 0$ for the rest of sites. The single hole impurity state of the Hamiltonian (4) at t' = 0 was studied previously by using exact diagonalization method for small clusters by Von Szczepanski et al. [7], Rabe and Bhatt [8], and Gooding [9]. The ground state was found to be orbitally doubly degenerate (S = 1/2) in certain parameter regime [8, 9, 10]. When the next n.n. hopping integral t' is included, our results below show that the doubly degenerate S=1/2 states is lowest in energy within a reasonable parameter range. The symmetry of the lowest energy state however is sensitive to boundary condition and parameters. In our calculations, we choose t = 1 and t = 0.3, suitable for the cuprates, and study the ground state as a function of t' and t = 0.3. We consider the clusters of 12- and 16-sites as illustrated in Fig. 2.

Exact diagonalization calculations of the t-t'-J model on small clusters have been reported [11, 12, 13, 14, 15, 16]. For a 16-(4×4) site cluster with periodic boundary condition

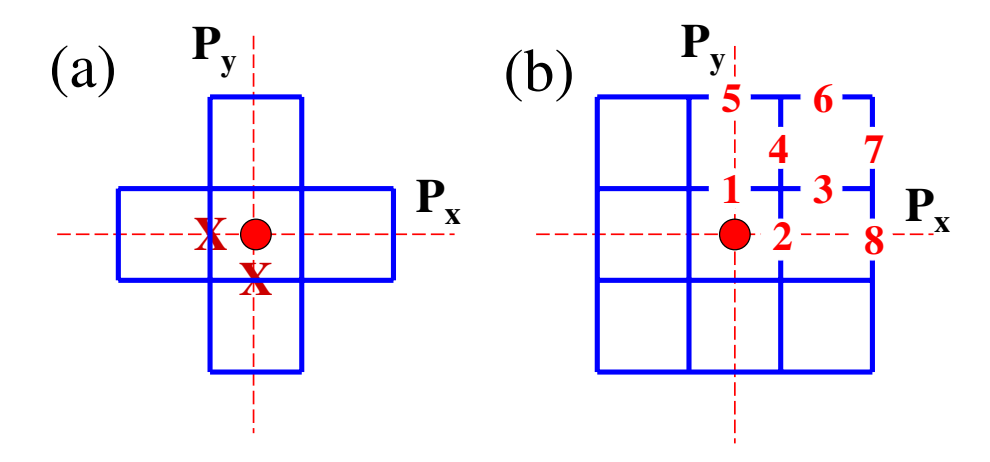


FIG. 2: The configuration of 12-site (a) and 16-site cluster (b). The dashed line corresponds to the reflection axis for $P_{x(y)}$. The red cross marks the tip position on the middle point of two n.n. Cu sites along the x- and y-axes. In (b), eight independent bonds are labeled with numbers.

(PBC), the ground state of a single hole has a four-fold symmetry with hole momentum $(\pm \pi/2, \pm \pi/2)$ if t' < 0, and a two-fold symmetry with hole momentum $(\pi, 0)$ or $(0, \pi)$ if t' > 0.

The presence of an impurity potential on the lightly doped t-J model affects not only the local charge and spin distributions but also the symmetry of the ground state wavefunction [7, 8, 9]. In this study, we focus on the reflection symmetries of a two-dimensional square lattice with respect to x- and y-axes passing through the sodium dopant (P_x and P_y respectively) and on the parity P_xP_y . Since $[P_{x(y)}, H] = 0$, we may classify states according to the quantum numbers of P_x , P_y . We denote the state with ($P_x = +1, P_y = +1$) as phase (I), and doubly degenerate state (+1, -1), and (-1, +1) as phase (II), and (-1, -1) as phase (III). In Fig. 3(a) and 3(b), we show the ground state phase diagram in terms of its reflection symmetry obtained by exact diagonalization. As we can see, there is a regime with the doubly degenerate ground state. Previous band structure calculation [17] and angle resolved photoemission experiments [18] both indicate a rather weak $t' \approx -0.1$ for $\text{Ca}_{2-x}\text{Na}_x\text{CuO}_2\text{Cl}_2$. Thus we expect the existence of doubly degenerate ground state in this doped material. We note that the four low-lying states with distinct reflection symmetries are very close in energy. Small perturbation of lattice geometry, boundary condition, t' or ϵ_s may change symmetry of the ground state. In Fig. 3(c), we show the energy level evolution

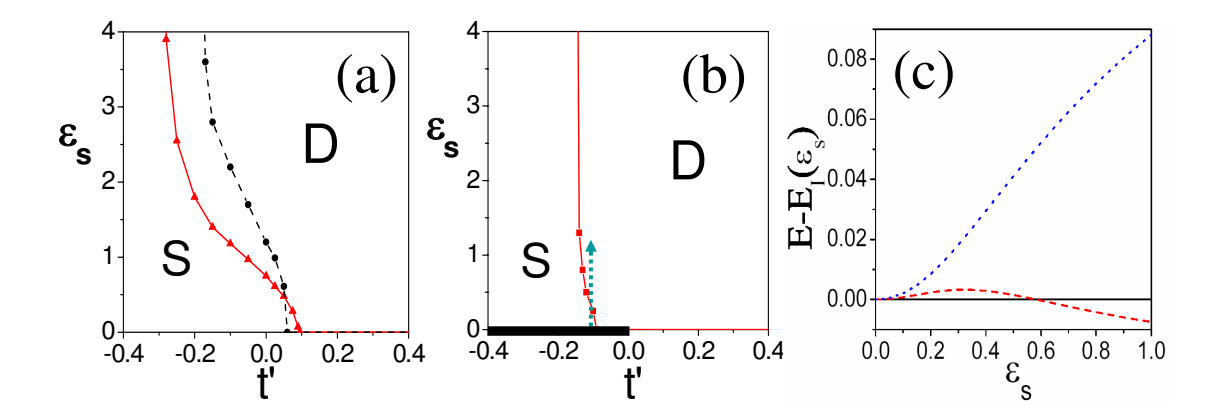


FIG. 3: Ground state phase diagram in the parameter space of the next n.n. hopping integral t' and the sodium impurity potential ϵ_s in (a) 12-site cluster (black solid line) and 16-site cluster (red dashed line) with open boundary condition, (b) 16-site cluster with PBC. Regime D: the doubly degenerate state; regime S: the singly degenerate state. The thick black line in (b) corresponds to the four-fold symmetric states at $\epsilon_s = 0$. (c) Energy levels as functions of ϵ_s at t' = -0.12 as indicated by the dashed green line in (b). E_I denotes the energy in phase I. The dashed line is for doubly degenerate states while the dotted line is for phase III.

as ϵ_s changes for a fixed value of t' = -0.12.

We next examine the effect of the rotational symmetry broken ground state to the STM measurements. We consider the system to be in one of the two degenerate states, say in the state of $P_x = 1, P_y = -1$. The broken symmetry may be caused by quadrupole interaction of two single-hole states or by other couplings. We remark that the local density of states at the Cu-sites remains rotational symmetric in this state. However, because of the interference of different Cu-sites to the integrated differential conductance in Eqn. (4), the STM tip at a position between two Cu-sites will break the rotational symmetry. To be specific, we consider the tip position above the two geometrically symmetric points at halfway between the Cu-site \vec{i} and its neighboring sites $\vec{i} + \hat{x}$ or $\vec{i} + \hat{y}$. The sodium impurity is located at $\vec{i} + \hat{x}/2 + \hat{y}/2$. Note that $\langle \vec{r} | \vec{i}, Cl \rangle = \langle \vec{r} | \vec{i} + \tau', Cl \rangle$ for the mid point \vec{r} , we obtain the expression for the integrated differential conductance $I^{x(y)}(\omega) = I(\frac{\hat{x}}{2}(\frac{\hat{y}}{2}), \omega)$ at position $\vec{i} + \frac{\hat{x}}{2}(\frac{\hat{y}}{2})$ with

the cut-off energy ω ,

$$I^{x(y)}(\omega) = \sum_{\sigma} I^{x(y)}_{\sigma}(\omega),$$

$$I^{x(y)}_{\sigma}(\omega) = A_0 \sum_{m} |\langle m| \sum_{\vec{\tau}} (-1)^{M_{\vec{\tau}}} (c^{\dagger}_{\vec{i}+\vec{\tau},\sigma} + c^{\dagger}_{\vec{i}+\hat{x}(\hat{y})+\vec{\tau},\sigma}) |\Psi^{1h}_{0}\rangle|^2 \Theta(\omega - E_m + E^{1h}_{0}), \quad (6)$$

where I_{σ} is the spin-dependent integrated differential conductance, and the Cu-site index \vec{i} has been dropped for simplicity. The conductance can be calculated in a small cluster. We diagonalize the hamiltonian H in Eqn. (5). exactly and find the ground state of the single hole and also all the eigenstates $|m\rangle$ and the corresponding energies E_m at the half-filling, which allows us to calculate all the matrix elements in Eqn. (6). Note that $I^x(\omega) = I^y(\omega)$ by symmetry if $|\Psi_0^{1h}\rangle$ is non-degenerate. In the parameter regime where $|\Psi_0^{1h}\rangle$ is doubly degenerate (see Fig. 2), I^x and I^y can be different. In Fig. 4(a), we plot $I^x(\omega)$ and $I^y(\omega)$ as functions of the cutoff energy ω obtained from the 12-site cluster calculations, where the hole groundstate has symmetry $P_x = +1$, $P_y = -1$ and has a spin $S_z = 1/2$. The asymmetry of I between the two tip scans is apparent and is more pronounced at a lower energy cutoff and becomes weaker at a high energy cutoff. To see the asymmetry more clearly, we also plot the ratio of the conductances at the two tip points in the same figure,

$$\eta(\omega) = I^x(\omega)/I^y(\omega). \tag{7}$$

It is interesting to note the strong cutoff energy dependence of the asymmetry in the conductance. For example, $\eta \approx 0.3$ for $\omega \approx J$, and $\eta \approx 0.85$ for $\omega = 4J$. At $\omega \to \infty$, $\eta \approx 1.04$, which shows a very weak asymmetry. Our theoretical results are consistent with the recent STM observation [1], where the strong asymmetry has been found at a lower energy 150 meV ($\sim J$), and the asymmetry becomes much weaker or unobservable at a high energy 600 meV ($\sim 4J$). In Fig. 4(b) and 4(c), we show the spin-dependent conductances $I_{\sigma}(\tau'/2,\omega)$ as functions of ω in different spin channels. Our theory predicts that the asymmetry is spin-dependent. At high energy cutoff limit, we find the ratio $I_{\uparrow}^x/I_{\uparrow}^y \sim 1.23$ in the spin-up channel and $I_{\downarrow}^x/I_{\downarrow}^y \sim 0.88$ in the spin-down channel. The asymmetry compensates each other in the two different spin channels, which gives a weaker asymmetry in the total ratio $I^x/I^y \sim 1.04$. We remark that rapid spin flip processes around the sodium impurity may make the spin-resolved STM experiments more difficult to observe. However, at very underdoped samples, the spin may be frozen around the sodium impurity, which should provide the possibility for the spin-resolved STM experiments.

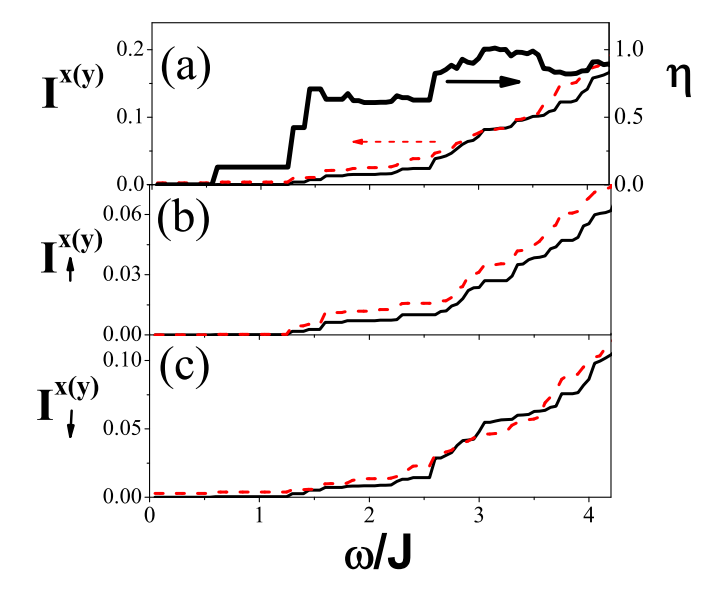


FIG. 4: The total integrated differential conductance on two cross (X) sites in Fig. 2a along the x(solid line) and along the y-axis (dashed line) as functions of the cut-off energy ω together with the
anisotropy ratio η (thick solid line). The results for spin-up channel (b), and spin-down channel
(c). In the calculations (b), and (c), the single hole state has a spin $S_z=1/2$.

To better understand our results, we analyze the groundstate and the conductance in a four-site cluster system. The 4-site cluster of the Hubbard model with a single hole was previously studied by Altman and Auerbach [19]. They have found that for not very large on-site Coulomb repulsion U, the ground state is two-fold degenerate with spin-1/2. We here study the single hole ground state of the Hamiltonian Eqn. (5), and focus on the spin-1/2 sector, which is relevant for not too small ratio of J/t. Note that the impurity potential does not play any role in the 4-site cluster. The ground state is doubly degenerate with the energy given by $E_g = -J/2 - \sqrt{3t^2 + (t' + J/2)^2}$, with $tan\gamma = \sqrt{3}t/(J + t' + E_g)$. The two degenerate states can be classified by symmetry $P_x = +1$, $P_y = -1$ and $P_x = -1$, $P_y = +1$. Assuming the former to be ground state, we find that apart from an overall prefactor, $I_{\uparrow}^x(\omega) = \frac{4}{3}\cos^2\gamma\Theta(\omega - J)$, $I_{\downarrow}^x(\omega) = \frac{2}{3}\cos^2\gamma\Theta(\omega - J)$, $I_{\uparrow}^y(\omega) = 0$ and $I_{\downarrow}^y(\omega) = \cos^2\gamma\Theta(\omega) + \sin^2\gamma\Theta(\omega - 2J)$. Due to the nature of the many body wavefunction, the conductance in Eqn.(6) may involve either destructive or constructive interference among different components. This effect is most drastic in I_{\uparrow}^y with an exact cancelation between them. Summing over spins, we have, $I^x(\omega) = I_{\uparrow}^x + I_{\downarrow}^x = 2\cos^2\gamma\Theta(\omega - J)$ while $I^y(\omega) = 1$

bond index	1	2	3	4	5	6	7	8
$\langle C_i^{\dagger} C_j \rangle$	0.342	0.328	0.122	0.129	0.020	0.014	0.012	0.016
$-\langle S_i S_j \rangle$	0.167	0.074	0.161	0.167	0.329	0.336	0.347	0.334

TABLE I: The hopping integral and spin-spin correlation function for various bonds in a 16-site cluster with PBC for t' = -0.1 and $\epsilon_s = 1.0$. The bond indices are labeled in Fig. 2(b).

 $\cos^2 \gamma \Theta(\omega) + \sin^2 \gamma \Theta(\omega - 2J)$. It is obvious that $\eta(\omega)$ becomes infinite for $\omega \in (0, J)$, $\eta(\omega) = 1/2$ for $\omega \in (J, 2J)$ while $\eta(\omega) = 2\cos^2 \gamma$ for $\omega > 2J$. At the limit of the large bias voltage, we have $\eta = 2\cos^2 \gamma$. For t'/t = -0.1, $\eta \sim 0.97$. Therefore, the asymmetry becomes rather weak with the increase of bias voltage. The ratio of the integrated conductances in the ground state with symmetry $P_x = -1$, $P_y = +1$ can be obtained by the interchange symmetry of x and y, and is given by $1/\eta$. We have also calculated the integrated conductance for the hole injection tunneling, and found also rotational asymmetric. The ratio of the conductances between the electron injected and hole injected is also asymmetric.

In the rotational symmetry broken state we considered above, the local charge density at each of four n.n. Cu sites around sodium dopant is uniform, but the n.n. Cu-Cu bondings are not equal. For instance, in the ground state with $P_x = +1$, $P_y = -1$ of the 16-site cluster, we show the expectation value of hopping integral $\langle C_i^{\dagger} C_i \rangle$ as well as spin-spin correlation function $\langle S_i S_j \rangle$ for various bonds, depicted in Table I. The hopping integral along bond 1 is slightly stronger than that of bond 2 while the spin-spin correlation function exhibits a much stronger asymmetry. The impurity may lead to localization of holes around this impurity which may result in a larger hopping integral and weaker spin-spin correlation function around this impurity. Close to the lattice boundary, since the hole density becomes very small for large impurity scattering strength, the spin-spin correlation function may approach to -0.34 and hopping integral vanishes. Our results are consistent with previous calculations. The strong variations of hopping integral and spin-spin correlation around the impurity may lead to the formation of local lattice distortion and the appearance of spin-lattice polaron due to the electron-phonon coupling [20], which may induce further rotational asymmetry. We speculate that this could be one of the reasons for the inhomogeneity in underdoped $Ca_{2-x}Na_xCuO_2Cl_2$.

The authors thank Y. Kohsaka and S. Davis for discussions of their experiments. YC

especially thanks P.W. Leung, T.K. Lee, H. Tsunetsugu, and M. Troyer for numerical assistance. YC and FCZ are supported by RGC grants from the Hong Kong SAR government, and TMR by the MANEP program of the Swiss Nationalfonds.

- [1] Y. Kohsaka et al., unpublished.
- [2] T. Hanaguri *et al.*, Nature **430**, 1001 (2004).
- [3] M. Randeria, R. Sensarma, N. Trivedi, and F.C. Zhang, Phys. Rev. Lett. 95, (2005) 137001.
- [4] P.W. Anderson, cond-mat/0406038.
- [5] T.M. Rice and H. Tsunetsugu, cond-mat/0509382.
- [6] J. Tersoff and D.R. Hamann, Phys. Rev. B **31**, 805 (1985).
- [7] K.J. Szczepanski, T.M. Rice, and F.C. Zhang, Europhys. Lett. 8, 797 (1989).
- [8] K.M. Rabe and R.N. Bhatt, J. Appl. Phys. **69**, 4508 (1991).
- [9] R.J. Gooding, Phys. Rev. Lett. **66**, 2266 (1991).
- [10] The double degenerate ground state was not found in Ref. [7], due to the lower symmetry of the cluster they considered.
- [11] E. Gagliano, S. Bacci, and E. Dagotto, Phys. Rev. B 42, 6222 (1990).
- [12] R.J. Gooding, K.J.E. Vos, and P.W. Leung, Phys. Rev. B 50, 12866 (1994).
- [13] A. Nazarenko, K.J.E. Vos, S. Haas, E. Dagotto, and R.J. Gooding, Phys. Rev. B 51, 8676 (1995).
- [14] M. Troyer, H. Tsunetsugu, and T.M. Rice, Phys. Rev. B 53, 251 (1996).
- [15] T. Xiang and J.M. Wheatley, Phys. Rev. B **54**, R12653 (1996).
- [16] C.T. Shih, Y.C. Chen, and T.K. Lee, Phys. Rev. B 57, 627 (1998).
- [17] L.F. Mattheiss, Phys. Rev. B 42, 354 (1990).
- [18] J.C. Ronning et al., Science **282**, 2067 (1998).
- [19] E. Altman and A. Auerbach, Phys. Rev. B 65, 104508 (2002).
- [20] P. Prelovsek, R. Zeyher, and P. Horsch, Phys. Rev. Lett. 96, 086402 (2006).